24th COBEM - 2017

24th ABCM International Congress of Mechanical Engineering
December 3-8, 2017, Curitiba, PR, Brazil

COBEM-2017-0937
NUMERICAL SOLUTIONS OF ELECTRO-OSMOTIC NEWTONIAN/NON-NEWTONIAN FLUID FLOWS

W. B. Souza
A. Castelo
Universidade de São Paulo, Instituto de Ciências Matemáticas e de Computação de São Carlos, SP, Brazil
wesley.bezerra@usp.br

A. M. Afonso
Faculdade de Engenharia da Universidade do Porto, Departamento de Engenharia Mecânica, Centro de Estudos de Fenómenos de Transporte (CEFT), Porto, Portugal
aafonso@fe.up.pt

Abstract. *The behavior of Newtonian and non-Newtonian fluids in microchannels was studied. To investigate the viscoelastic fluid flow, the constitutive rheological model of Phan-Thien-Tanner was used. Furthermore, electrokinetic effects will be analyzed and the full Phan-Thien-Tanner single mode was studied. The flow is influenced by the action of an applied external electric field and the behavior of this system as a whole studied through numerical simulations performed in a new system named HiG-Flow. For computations, the finite differences method is used and stabilization techniques were employed to solve the constitutive equation and then determine the solution of the fluid flow. The Debye-Hückel approach was applied to solve the electro-osmotic flow. The influence of the applied external field on the stress and velocity profile will shown and the results will be discussed.*

Keywords: *Finite Differences, HiG-Flow, Viscoelastic Flows, Electro-osmotic Flows*

1. INTRODUCTION

In microfluidics, small volumes of fluid are manipulated, and the microfluidic devices require small amounts of sample, enabling the execution of a particular process in short time. Thus, the Lab-on-a-chip (Persat et al., 2009) technology reduces the experimental configuration in a laboratory by a scale factor equal to 1000 or more, ranging from scales of one decimeter to one hundred micrometers . This reduction in one dimension is equivalent a factor of 10^9 in three dimensions, that is, considering a volume of 1 L, this would be reduced to 1 nL. This configuration is of great relevance concerning application in science and technology, such as medicine, biology and engineering (Whitesides, 2006). Miniaturized systems for delivery of therapeutic agents, drug detection or DNA molecules, microchemical reactors are some examples of applications in microfluidics. Thus, several studies have been performed in microfluidics, and the relevance of the important applications attracts several researchers.

The electrokinetic effects in an electrolytic fluid are studied in this work, in particular the electro-osmosis, being this a subject that allows the exchange of information of researchers from different areas, such as chemistry, physics, engineering and applied mathematics. The electrolyte flow is induced due the application of an external electric field between the inflow and outflow. This flow occurs due to the formation of ion layers near the channel walls, and the movement of these charges near the walls causes a moviment of the neutral core fluid which are dragged into the channel. Several studies on electro-osmotic flow were performed, from the analytical solution of newtonian fluid, arriving at the present time with numerical solutions for non-newtonian models. The aim of this work is to study the phenome of micro-scale flows, in particular using the HiG-Flow system to study electro-osmotic flows of non-Newtonian fluids, showing the influence of the Deborah number on the behavior of the flow.

2. PROBLEM DESCRIPTON

2.1 Governing equations

To be more general, we will describe the non-newtonian problem without specifying which the constitutive model to be used. The HiG-Flow system works in this way, allowing an immediate implementation of the constitutive model to be used without affecting other models already implemented, in other words this system allows us to simulate several

constitutive models (Castelo et al., 2017). In the next section we will focus on the solution of linear Phan-Thien/Tanner model (LPTT). Assuming the fluid incompressible laminar and isothermal flow, the governing equations that we desire to solve for the electroosmotic problem are given by:

$$\nabla \cdot \mathbf{u} = 0, \tag{1}$$

$$\frac{\partial \mathbf{u}}{\partial t} + \mathbf{u} \cdot \nabla \mathbf{u} = -\nabla p + \frac{1}{Re}\nabla^2 \mathbf{u} + \nabla \cdot \mathbf{S} + \mathbf{F}, \tag{2}$$

$$\mathbf{T} = \frac{2(1-\beta)}{Re}\mathbf{D} + \mathbf{S}, \tag{3}$$

where $\mathbf{u}$ is the velocity field, t is time, p is the pressure, $Re = \rho U H/\eta_0$ is the Reynolds number, U is the average velocity, H is the channel height, ρ the mass density and η_0 denotes the total shear viscosity $\eta_0 = \eta_s + \eta_p$. The rate of deformation tensor $\mathbf{D} = \frac{1}{2}\left(\nabla \mathbf{u} + (\nabla \mathbf{u})^T\right)$ and $\mathbf{T}$ is the elastic stress. The dimensionless solvent viscosity coefficient is given by $\beta = \frac{\eta_s}{\eta_0}$. The evolution in time of the polimeric stress tensor is related by

$$\frac{\partial \mathbf{T}}{\partial t} + (\mathbf{u} \cdot \nabla)\,\mathbf{T} - \left[(\nabla \mathbf{u})^T \cdot \mathbf{T} + \mathbf{T} \cdot \nabla \mathbf{u}\right] = \frac{1}{De}\mathbf{M}(\mathbf{T}) \tag{4}$$

where $De = \lambda U/H$ is the Deborah number and λ is the relaxation time of the fluid. Here we will be use a kernel conformation tensor (Fattal and Kupferman, 2004, 2005; Afonso et al., 2012b) and then determine the stress tensor. An alternative form to describe viscoelastic models is by using the conformation tensor, $\mathbf{A}$. This tensor is symmetric and positive definite which is an important mathematical property for the construction of matrix transformations and/or decompositions. In general the equation for $\mathbf{A}$ can be written as

$$\frac{\partial \mathbf{A}}{\partial t} + (\mathbf{u} \cdot \nabla)\,\mathbf{A} - \left[\mathbf{A}\nabla \mathbf{u} + \nabla \mathbf{u}^{\mathbf{T}}\mathbf{A}\right] = \frac{1}{De}\mathcal{M}(\mathbf{A}), \tag{5}$$

where $\mathcal{M}(\mathbf{A})$ is define according to the viscoelastic model.

A problem that challenges many researchers in computational rheology is to solve the Eq. (4) - or Eq. (5) - for high values of Deborah number De. This problem occurs because all numerical methods are unstable for certain critical values of De. In order to overcome such failure, Fattal and Kupferman (Fattal and Kupferman, 2004) proposed a reformulation of the differential constitutive equations into a equation for the matrix-logarithm of the conformation tensor. Extending the ideas proposed by Fattal and Kupferman (Fattal and Kupferman, 2004, 2005), Afonso et al. (Afonso et al., 2012b) presented a generic kernel-conformation tensor transformation that allows apply differents kernel functions to the matrix transformation, in which the evolution equation for $\Bbbk(\mathbf{A})$, can be expressed in its tensorial formulations as

$$\frac{\partial \Bbbk(\mathbf{A})}{\partial t} + (\mathbf{u} \cdot \nabla)\,\Bbbk(\mathbf{A}) = \mathbf{\Omega}\Bbbk(\mathbf{A}) - \Bbbk(\mathbf{A})\mathbf{\Omega} + 2\mathbb{B} + \frac{1}{De}\mathbb{M} \tag{6}$$

where $\mathbb{B}$ and $\mathbb{M}$ are symmetric tensors constructed by the orthogonalization of the diagonal tensors.

Thus, the HiG-Flow system solves Eq. (6) instead of Eq. (4), for more details please see (Castelo et al., 2017). Considering the Newtonian fluid flow, the tensor $\mathbf{S}$ is null and the velocity and pressure are only updated at each step of time. For the numerical simulations, the HiG-Flow has different modules to march in time for the newtonian case as for the solution of the non-newtonian case.

2.2 Phan-Thien/Tanner model

Here we are interested in the LPTT model to solve the constitutive equation and then determine the velocity field. For this model, the right hand side of the Eq. (4) can be written as:

$$\mathbf{M}(\mathbf{T}) = \frac{2(1-\beta)}{Re}\mathbf{D} - \left(1 + \frac{\varepsilon\, Re\, De}{1-\beta}\mathrm{tr}(\mathbf{T})\right)\mathbf{T} - \xi\, De\,(\mathbf{T} \cdot \mathbf{D} + \mathbf{D} \cdot \mathbf{T}). \tag{7}$$

The dimensionless parameter ε is related to the steady-state elongational viscosity in extensional flows and ξ is a parameter relationated with the molecular slip. If ξ is null, the model reduces to the simplified PTT (sPTT). On the other hand if ξ is not null, there will be a non-zero second normal-stress difference in shear, leading to secondary flows in ducts

having non-circular cross-sections, which is superimposed on the streamwise flow (Phan-Thien, 1978). In fact the right hand side for the conformation tensor Eq. (5)is given by

$$\mathcal{M}(\mathbf{A}) = \left(1 + \frac{\epsilon\, Re\, De}{1-\beta}\mathrm{tr}\,(\mathbf{S})\right)(\mathbf{I}-\mathbf{A}) - 2\xi\, De\,(\mathbf{B}-\mathbf{BA}) \tag{8}$$

In this way the equations of motion are solved for the LPTT model fluid flow.

2.3 Electro-osmotic forces in a channel

Electro-osmotic fluid flows were studied in two different problems, namely: Newtonian fluid flow subjected to electro-osmotic forces and Non-newtonian fluid flow subjected to electro-osmotic forces. Figure 1 shows the flow of a fluid between two parallel plates.

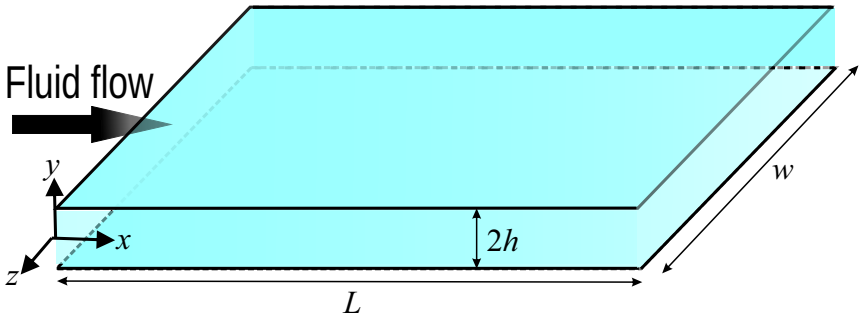

Figure 1. Illustration of the channel used to perform the electro-osmotic fluid flows.

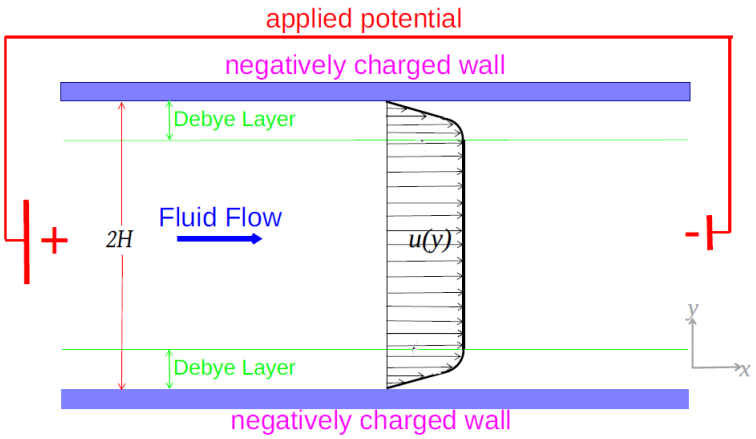

Figure 2. Geometry of the microchanel used to study the electro-osmotic fluid flow.

The schematic representation of electro-osmotic flow is show in Fig 2. The applied potential along the axis of the channel provides the driving force necessary to occur the electro-osmotic flow.

The LPTT constitutive model (Thien and Tanner, 1977) was used for studies involving electro-osmotic flow of non-Newtonian fluids. The channel used has the same dimensions for the two problems mentioned above. In fact, numerical simulations are performed in two dimensions, taking into account $L, w >> H$, where H is the channel height. Moreover, due to the symmetry of the problem, we analyzed only half of the channel, that is $0 \leq y \leq H$.

For the problems subjected to the electro-osmotic forces, there exists a source term in Eq. (2), $\mathbf{F} = \rho_e \mathbf{E}$, where $\mathbf{E}$ is the electric field , which is given by the external applied potential gradient $\mathbf{E} = -\nabla\phi$. In fact, one of the problems studied in this paper refers to a PTT model fluid flow without the action of external forces, that is, $\mathbf{F} = 0$. The electric field appears due to two contributions, one is the applied potential ϕ and the other due to the induced potential ψ which changes in the transversal direction to the channel walls. Thus, $\mathbf{E} = \nabla\phi + \nabla\psi$. The formation of the Debye layer occurs due to the spontaneous movement of the charged species near the channel wall, causing a charge redistribution in the fluid that originates the electrical double layer (Grahame, 1947). Therefore, the equations to be solved for the source term are given by

$$\nabla^2\phi = 0 \tag{9}$$

$$\nabla^2\psi = -\frac{\rho_e}{\epsilon} \tag{10}$$

where ϵ is the dielectric constant of the solution. In this work we will consider that there is no interference between the two electrical contributions, that is, the external field applied is much smaller than the transversed induced field. Assuming that the flow conditions obey the Debye-Hückel approuch, and taking into account that the flow occurs in the direction x,

$$\frac{d^2\psi}{dy^2} = \kappa^2\psi \tag{11}$$

where $\kappa = 1/\lambda_D$ is the Debye-Hückel parameter related to the Debye layer thickness λ_D. These approximations are valid for values of $10 \leq \kappa H \leq 10^3$, so this means that this problem is governed by induced potential energy that does not exceed the value of the thermal energy (Fixman, 1979). The solution of Eq. (11) and for the distribution of charges in the electrokinetic equilibrium are

$$\bar{\psi} = \frac{\cosh(\bar{\kappa}\bar{y})}{\cosh(\bar{\kappa})} \tag{12}$$

$$\rho_e = -\epsilon\zeta_0\kappa^2\frac{\cosh(\bar{\kappa}\bar{y})}{\cosh(\bar{\kappa})} \tag{13}$$

where ζ_0 is the zeta potential at the wall, and here we defined the non-dimentional quantities $\bar{\psi} = \psi/\zeta_0$ is the adimentional induced potential $\bar{\kappa} = \kappa H$ and $\bar{y} = y/H$. Complete solutions for this problem can be found in more detail in (Afonso et al., 2009; Dhinakaran et al., 2010).

3. Numerical procedures

The computational domain to the simulation is obtained through HiG-Tree, which generates a hierarchical mesh. In our bi-dimentional case, this mesh is a generalized quad-tree (Finkel and Bentley, 1974). In general, hierarchical meshes impose difficulties in the numerical scheme based on cartesian approximations, and requires the use of spatial interpolations at unknown points of the stencil. The interpolations of the properties in the center of the faces and in the center of the cells are made by the technique of moving least squares, which uses a given set of points where the property is known to estimate a unknown value in a neighbor point. Differential equations are discretized by the method of finite-differences. Solvers using the PETSc library (Portable, Extensible Toolkit for Scientific Computation) (Balay et al., 2017) are used to solve linear systems (Castelo et al., 2017). Results were obtained through numerical simulations using a Core i7 2.4 GHz CPU, 16 Gb memory. The mesh with refinements along the channel were obtained using HiG-Tree. The total length of the mesh is $20H$. Better results were obtained with $\Delta x/\Delta y = 4$. Near the walls the minimum size is $\Delta y_{min}/H = 7.8125 \times 10^{-4}$ and $\Delta x_{min}/H = 3.1250 \times 10^{-3}$. Figure 1 shows the mesh used to simulate the electro-osmotic flows.

4. RESULTS

The results obtained for the tree problems will be presented in this section. Due to the symmetry of the problems, the results will be presented considering only the positive part of the channel relative to its axis.

4.1 Poiseille flow of a sPTT fluid (F = 0)

For this problem, the sPTT model was solved using the HiG-Flow system and the results compared with literature for this type of rheological model. For these tests we vary the coefficient of viscosity β. Note that if $\beta \to 1.0$, the flow tends to have Newtonian behavior. For pure polimeric flow, namely $\beta = 0.0$, the result tends towards the Oldroyd-B model as show for (Cruz et al., 2005) and the influence of the Deborah number can be found in (Oliveira and Pinho, 1999). We observe the behavior of velocity and stresses in the flow. Related results and analytical expressions can be found in (Cruz et al., 2005). Figure 4 shows the velocity of the fluid within the pipe, according to the viscosity coefficient. For $\beta = 0.8$,

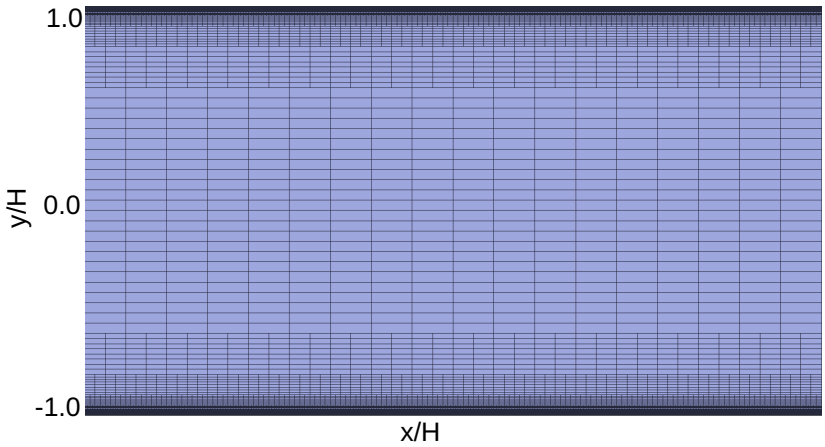

Figure 3. Computational grid used to perform the electro-osmotic fluid flows. The mesh is in scale. At center of the grid $\Delta x/H = 0.2$.

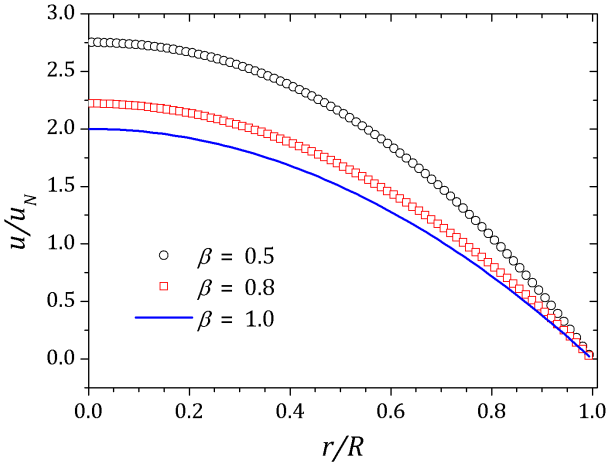

Figure 4. Pipe flow of sPTT model. Velocity profiles at different values of viscosity coefficient β. $De = 1.0$, $\varepsilon = 0.25$.

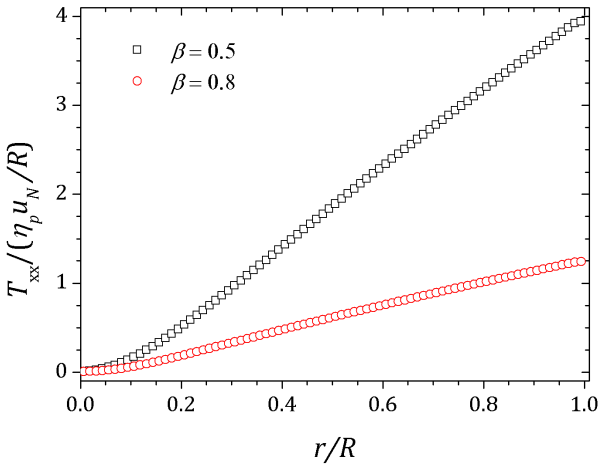

Figure 5. Pipe flow of sPTT model. Normal stress for different values of viscosity coefficient β. $De = 1.0$, $\varepsilon = 0.25$

the velocity profile is approximately newtonian, and if β decreases the average velocity increases. The scaled velocity $u_N = -\dfrac{R^2}{8\eta_0}\dfrac{dp}{dx}$ can be understood as the average velocity of a Newtonian fluid.

The variation of the normal stress in the fluid flow is shown in Fig. 5 and the shear stress is shown in Fig 6. The curves

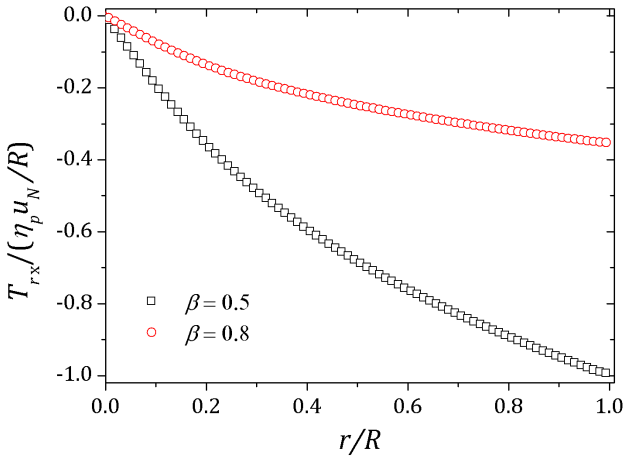

Figure 6. Pipe flow of sPTT model. Shear stress for different values of viscosity coefficient β. $De = 1.0$, $\varepsilon = 0.25$

are scaled by the factor $\eta_p u_N/R$. Increasing the polymer viscosity η_p which means decrease β, both normal stress and shear stress increase. Near the pipe axis, the normal stress vary more slowly, and increasing r, T_{xx} increases linearly.

4.2 Newtonian fluid flow subjected to electro-osmotic forces

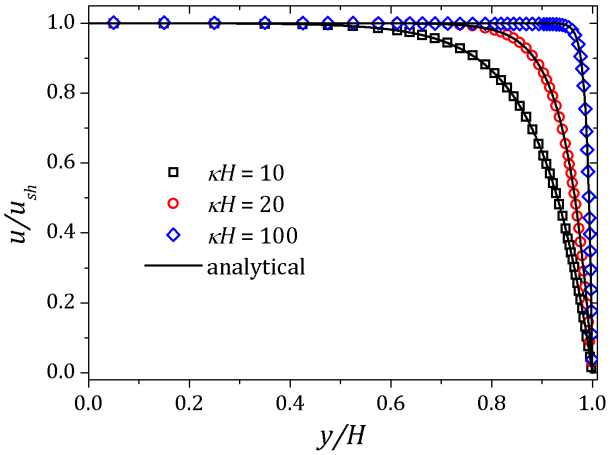

Figure 7. Velocity profiles for the newtonian fluid flow subjected to electro-osmotic forces in a channel. Effect of different kH.

In the case of a Newtonian fluid, the effect of the electric force makes the velocity profile depends on the distance of the channel wall and the thickness of the Debye layer relative to the channel size, that is, the parameter $\bar{\kappa} = \kappa H$ (Burgreen and Nakache, 1964). The thinner the Debye layer, the higher the charge concentration near the walls and the higher the velocity variation, so an adaptive mesh with grid refinement must be applied near the walls. Figure 7 shows the velocity profile for three different values of $\bar{\kappa}$. Note that the higher $\bar{\kappa}$, the smaller the thickness of the Debye layer, causing a sharp effect to the velocity profile near the wall. The scaled factor $u_{sh} = -\epsilon\zeta_0 E_x/\eta$ is the Helmholtz-Smoluchowski velocity (Park and Lee, 2008).

For ilustrate the velocity profile convergence was used three different grids. The main difference is the grid refinement, increasing the refinement near the walls to improve convergence. Effect of mesh refinament is show in Fig 8. Note that for the mesh with $\Delta y_{min}/H = 2.5000 \times 10^{-2}$ the nearest point the wall is clearly outside the expected curve. Increasing refinement, $\Delta y_{min}/H = 3,1250 \times 10^{-3}$, all points remain within the analytical curve, but there are spaces with no points due the sharp effect near the wall and for $\Delta y_{min}/H = 7.8125 \times 10^{-4}$ these spaces were filled and then the simulated curve agrees with analytical curve.

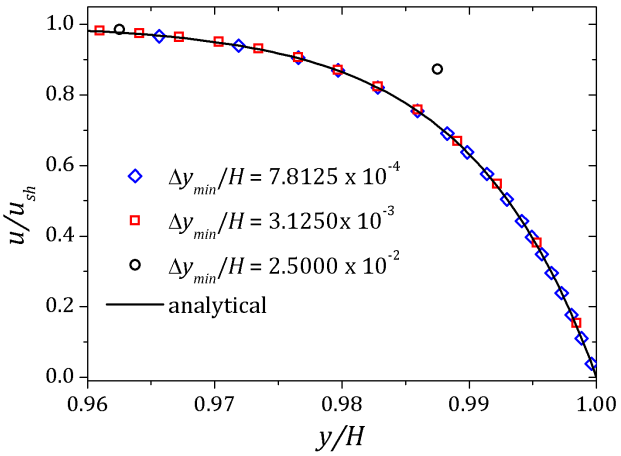

Figure 8. Effect of mesh refinament. Velocity profile of a newtonian fluid subjected to electro-osmotic forces in a channel. We fixed $kH = 100$ and vary the refinament near the wall. Image is zoomed near the wall to improved visualization of the refinament.

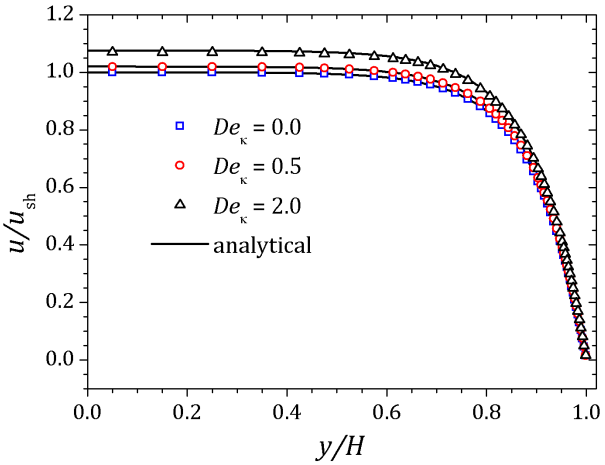

Figure 9. Velocity profiles for the non-newtonian fluid flow subjected to electro-osmotic forces in a channel. Here we fixed $\varepsilon = \xi = 0.01$ and $\kappa H = 10$.

4.3 Non-newtonian fluid flow subjected to electro-osmotic forces

The LPTT model was used to solve this problem. Therefor the velocity depends on y and $\bar{\kappa}$ it will also vary according to the relaxation time of the fluid. In this way, the velocity profile is affected by the Deborah number $De_\kappa = \lambda \kappa u_{sh}$ (Afonso et al., 2009, 2012a), as shown in Fig. 9. For this problem we set $De_\kappa = 0.5$ and $De_\kappa = 2.0$. In addition, the parameters $\xi = \varepsilon = 0.01$ were fixed. The Debye parameter assumed two different values, $\bar{\kappa} = 10$ and $\bar{\kappa} = 100$. For low Deborah number $De_\kappa = 0.5$, the velocity profile indicates behavior similar to that of a newtonian fluid. Increasing the number of Deborah is apparent the changes on velocity profile respecting to the Newtonian profile due to the low viscosities near the wall, in fact influenced by the appearance of the shear stress of the LPTT model. The normal and shear stress are shown in Fig. 10 and Fig. 11, in which we can observe that the numerical results are similar to the analytical solution.

5. CONCLUSION

The HiG-Fow system was used for numerical simulation of newtonian and viscoelastic flows in microchannels. This solver system has some constitutive models implemented, among them the LPTT that was used in this study. The flow governed by this constitutive model was studied and the computational results obtained indicate that the method used can be applied to solve related problems.

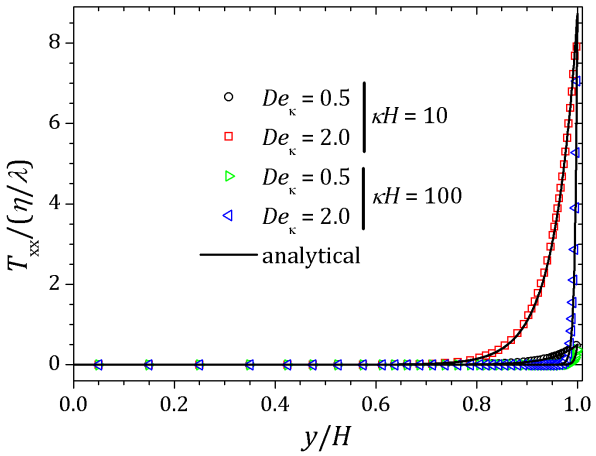

Figure 10. Normal stress for $De_\kappa = 0.5$ and $De_\kappa = 2.0$ at $\kappa H = 10$ and $\kappa H = 100$. We fixed $\varepsilon = \xi = 0.01$.

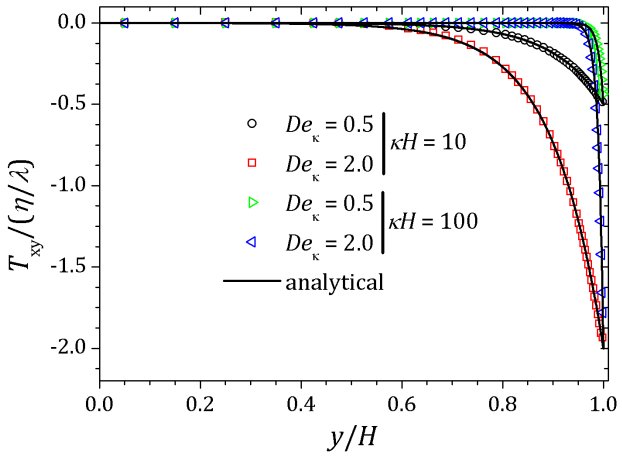

Figure 11. Shear stress for $De_\kappa = 0.5$ and $De_\kappa = 2.0$ at $\kappa H = 10$ and $\kappa H = 100$. We fixed $\varepsilon = \xi = 0.01$.

The effect of the applied electric field was investigate and the numerical results obtained and then compared with analytical and numerical results already existent in the literature for the problem. The Debye-Hückel approximation was used. For non-Newtonian fluid, the velocity profile depends on the distance to the wall channel, the Deborah number, and the size of the Debye layer. Adaptive meshes were used due to necessary refinement near electrically charged boundaries. This is one of the major problems with respect to the simulation time of flows subject to electro-osmotic forces. Interpolations are made because the mesh is not homogeneous and the solution becomes increasingly expensive. The use of a regular mesh without refinements becomes very expensive with respect to the time machine required to the simulation.

6. ACKNOWLEDGEMENTS

The authors acknowledge the financial support given Fapesp under project CEPID under process 2013/07375-0. A. Castelo acknowledge CNPq process 305923/2003-7. A. M. Afonso acknowledge the support by CEFT (Centro de Estudos de Fenómenos de Transporte) and the funding by FCT (Fundação para a Ciência e Tecnologia) through project PTDC/EMS-ENE/3362/2014. W. B. Souza acknowledge the support given by FACET-UFGD (Faculdade de Ciências Exatas e Tecnologia da Universidade Federal da Grande Dourados).

7. REFERENCES

Afonso, A., Alves, M., and Pinho, F. (2009). Analytical solution of mixed electro-osmotic/pressure driven flows of viscoelastic fluids in microchannels. *Journal of Non-Newtonian Fluid Mechanics*, 159(1):50–63.

Afonso, A., Pinho, F., and Alves, M. (2012a). Electro-osmosis of viscoelastic fluids and prediction of electro-elastic flow

instabilities in a cross slot using a finite-volume method. *Journal of Non-Newtonian Fluid Mechanics*, 179:55–68.

Afonso, A., Pinho, F., and Alves, M. (2012b). The kernel-conformation constitutive laws. *Journal of Non-Newtonian Fluid Mechanics*, 167:30–37.

Balay, S., Abhyankar, S., Adams, M. F., Brown, J., Brune, P., Buschelman, K., Dalcin, L., Eijkhout, V., Gropp, W. D., Kaushik, D., Knepley, M. G., McInnes, L. C., Rupp, K., Smith, B. F., Zampini, S., Zhang, H., and Zhang, H. (2017). PETSc Web page.

Burgreen, D. and Nakache, F. (1964). Electrokinetic flow in ultrafine capillary slits1. *The Journal of Physical Chemistry*, 68(5):1084–1091.

Castelo, A., Afonso, A., and Souza, W. (2017). A finite difference method in hierarquical grids for viscoelastic fluid flow simulations. *In preparation*.

Cruz, D., Pinho, F. T. d., and Oliveira, P. (2005). Analytical solutions for fully developed laminar flow of some viscoelastic liquids with a newtonian solvent contribution. *Journal of non-newtonian fluid mechanics*, 132(1):28–35.

Dhinakaran, S., Afonso, A., Alves, M., and Pinho, F. (2010). Steady viscoelastic fluid flow between parallel plates under electro-osmotic forces: Phan-thien–tanner model. *Journal of colloid and interface science*, 344(2):513–520.

Fattal, R. and Kupferman, R. (2004). Constitutive laws for the matrix-logarithm of the conformation tensor. *Journal of Non-Newtonian Fluid Mechanics*, 123(2):281–285.

Fattal, R. and Kupferman, R. (2005). Time-dependent simulation of viscoelastic flows at high weissenberg number using the log-conformation representation. *Journal of Non-Newtonian Fluid Mechanics*, 126(1):23–37.

Finkel, R. A. and Bentley, J. L. (1974). Quad trees a data structure for retrieval on composite keys. *Acta Informatica*, 4(1):1–9, doi:10.1007/BF00288933.

Fixman, M. (1979). The poisson–boltzmann equation and its application to polyelectrolytes. *The Journal of Chemical Physics*, 70(11):4995–5005.

Grahame, D. C. (1947). The electrical double layer and the theory of electrocapillarity. *Chemical reviews*, 41(3):441–501.

Oliveira, P. J. and Pinho, F. T. (1999). Analytical solution for fully developed channel and pipe flow of phan-thien–tanner fluids. *Journal of Fluid Mechanics*, 387:271–280.

Park, H. and Lee, W. (2008). Helmholtz–smoluchowski velocity for viscoelastic electroosmotic flows. *Journal of colloid and interface science*, 317(2):631–636.

Persat, A., Suss, M. E., and Santiago, J. G. (2009). Basic principles of electrolyte chemistry for microfluidic electrokinetics. part ii: Coupling between ion mobility, electrolysis, and acid-base equilibria. *Lab Chip*, 9:2454–2469, doi:10.1039/B906468K.

Phan-Thien, N. (1978). A nonlinear network viscoelastic model. *Journal of Rheology*, 22(3):259–283.

Thien, N. P. and Tanner, R. I. (1977). A new constitutive equation derived from network theory. *Journal of Non-Newtonian Fluid Mechanics*, 2(4):353–365.

Whitesides, G. M. (2006). The origins and the future of microfluidics. *Nature*, 442(7101):368–373.

8. RESPONSIBILITY NOTICE

The authors are the only responsible for the printed material included in this paper.